Solid-state polymerization of a diacetylene studied by neutron scattering

H. Grimm* and J. D. Axe
Brookhaven National Laboratory, Upton, New York 11973

C. Kröhnke
Institut für Makromolekulare Chemie, Universität Freiburg, 7800 Freiburg, Federal Republic of Germany

(Received 22 July 1981)

The solid-state polymerization process of a diacetylene is investigated by neutron scattering. In contrast to x rays, neutrons do not induce polymerization and a detailed examination is possible in the autocatalytic region of the thermally activated polymerization process. In this region there appear diffuse sheets of diffracted intensity, split into doublets, which correspond to the one-dimensional propagation of the conversion. The Bragg reflections broaden, decrease, and also display multiple peaks. An Ising model for the limit of uncorrelated chains is compared to experiment. Above the 50%-conversion level the onset of chain interaction becomes visible. Preliminary data were obtained concerning the behavior of acoustic phonons and the structural phase transformation under the influence of polymerization.

I. INTRODUCTION

Molecular crystals of diacetylenes may undergo a solid-state polymerization process[1] as indicated in Fig. 1(b).[2] The figure shows the formation of a covalent bond between the diacetylene molecules. Favorable spatial arrangement of the molecules provides that even large crystals "survive" the strain resulting from the formation of the new covalent bonds and that the polymerization process may be induced by thermal and radiation energy. The strain leads to a strong pressure dependence of polymer chain growth.[3] The availability of large deuterated crystals of the best investigated member of the diacetylene family makes possible the study of the polymerization process with neutron scattering. This compound, with the monomeric formula $R-C\equiv C-C\equiv C-R$ (see Fig. 1) with

R representing $CD_2-O-SO_2-\langle\bigcirc\rangle-CD_3$,

is named bis (p-toluene sulfonate) of 2,4-hexadiyne-1,6-diol, abbreviated by TS and by PTS in the polymer state. We will use PTS throughout the paper regardless of the state of polymerization of the crystal. Fortunately, neutrons do not induce polymerization. Thus one may follow the conversion from the monomer to the polymer state in small steps, which is important since there occurs a drastic "speed up" of the reaction for conversion greater than about 10%. This S-shaped conversion curve[4] is depicted in Fig. 2. The activation energy of about 1 eV gives rise to the strong dependence of the time scale of the process on the temperature of the crystal as indicated by the different abscissas of Fig. 2. This dependence allows the polymerization process to be "stopped" by cooling. The interested reader is referred to the review

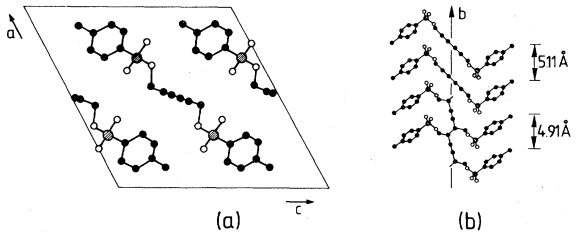

FIG. 1. (a) (High temperature) structure of PTS projected along ⟨010⟩ axis. (b) Projection of TS molecules onto the "backbone" plane in the monomer and polymer state (●) C, (○) O (▨) S, H not shown.

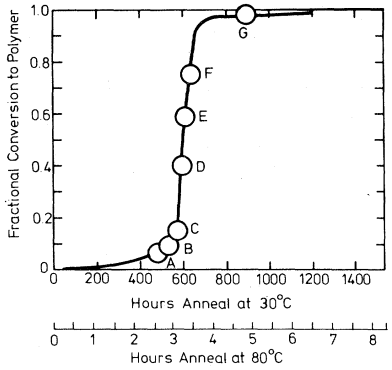

FIG. 2. Time dependence of conversion to the polymer state for PTS for two temperatures (Ref. 4). See Ref. 7 for a discussion of the effect of deuteration and temperature on the length of the induction period and the slope in the autocatalytic region, respectively. The symbols A and G mark the estimated states for the investigation of crystal number 3.

article of Wegner[5] for additional information about the solid-state polymerization, which has been deduced from calorimetric, optical, x-ray, and ESR measurements.

From what is said, the process of polymerization should give rise (i) to a change in the forces due to the formation of the intermolecular covalent bond, (ii) to a change of the "lattice constants" due to the reduction of the intermolecular distance, and (iii) to diffuse elastic scattering due to the disorder in the partially converted crystal.

With diffuse x-ray scattering[6] a sheetlike structure of the disorder scattering has been observed which corresponds to an essentially one-dimensional propagation of the polymerization process or in other words to only weak coupling perpendicular to this dimension (the crystallographic b direction, see Fig. 1).

We have studied these three topics by neutron scattering. A peculiar difficulty of the measurements has been the limited number of large monomer crystals in conjunction with the irreversibility of the polymerization process. Therefore, a systematic quantitative investigation of the polymerization dependence of several interesting properties has to be postponed for future experiments.

I. EXPERIMENTAL

By methods described elsewhere[7] one of us (C.K.) succeeded in growing large deuterated single crystals of PTS. The deuterated compound was chosen to minimize the incoherent scattering caused by hydrogen, which would otherwise appear as huge "background", resulting in a poor signal-to-noise ratio. Three crystals have been used with volumes of 0.1, 0.3, and 0.4 cm^3. In the initial state, the crystals were transparent rosy, indicating that they were already polymerized to some degree—presumably due to imperfect cooling during transportation. The crystals were wrapped in Al foil, the foil glued to a thin Al sample holder, the holder mounted and sealed under He atmosphere into a standard sample chamber which in turn was attached to the cooling surface of a *CT*14 bath cryostat. This procedure ensures good temperature homogeneity throughout the sample volume, which is important for a homogeneous polymerization of the crystal. The experimental procedure consisted of a sequence of annealing (hours at about 330 K) and measuring (days at about 200 K) periods. Preliminary measurements with the 0.1-cm^3 crystal were performed on the triple-axis spectrometer *SV*4 in Jülich. They showed no difference in the lattice constant b (sensitive to the degree of conversion) before and after a measuring period, thus indicating that the γ-radiation level within the neutron beam does not alter significantly the degree of conversion.

With better statistics, a second series of experiments was undertaken with the 0.3- and the 0.4-cm^3 crystals. Those measurements were performed at the Brookhaven High Flux Beam Reactor. Pyrolytic graphite was used for both the monochromator and analyzer of the triple-axis spectrometer. An initial neutron energy of about 14 meV in conjunction with an aligned pyrolytic graphite filter was chosen to avoid contamination of the beam from higher-order scattered neutrons.

Three states of polymerization of the 0.3-cm^3 crystal were investigated in the $(hk0)$ plane. The degree of conversion which characterizes these three states could be determined from the conversion dependence of the lattice parameter b obtained by x rays[8] at 120 K. According to this calibration curve, the different states correspond to about 13%, 19%, and 60% conversion of the crystal into the polymer state. In what follows we shall refer to these as the first, second, and third polymerization states, respectively.

The comparison of these three states revealed the following tendencies with increasing conversion ($\leq 60\%$).

A. Bragg reflections

The peak intensities of the Bragg reflections decrease rapidly. Inspection of the width parallel and perpendicular to the reciprocal-lattice vector shows that this reduction is mainly due to an increasing "mosaic" width, which reflects the stressed state of the crystal. In addition, the lattice parameter b (along with the polymerization process proceeds) first shifts to smaller values and is asymmetrically broadened at 60% conversion. In fact, monitoring the (020)-reflection during polymerization from state two to three, the Bragg-peak vanished smoothly in the background and a new weak reflection was observed at a position which corresponds to reduction of b by about 4.5%.

B. Diffuse sheets

The first state (about 13% conversion) shows weak indications of the diffuse sheets [see Fig. 3(a)]. An estimate of the "thickness" of the sheets is $0.08b^*$ which corresponds to a correlation length of about $2b$ or the extension of a dimer molecule. Yet this value should rather be taken as a rough order of magnitude, taking into account the small signal to "background" ratio. The strong enhancement of the sheet intensity which has occurred by about 60% conversion is demonstrated in Fig. 3(b). The sheets become thin and the width of the "profile" scans is given by the instrument resolution. All three curves in Fig. 3 of the profile in this state [similar scans at $(3.4, 2 \pm 0.3, 0)$ and $(3.4, 3 \pm 0.3, 0)$] show asym-

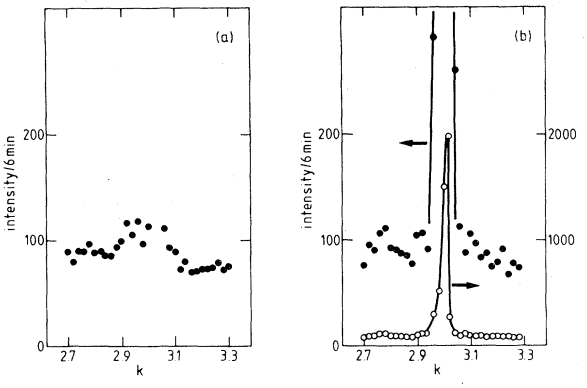

FIG. 3. (a) Scan across the position of the third sheet $(0.3,k,0)$ for about 13% conversion (220 K). (b) The same as (a) at about 60% conversion.

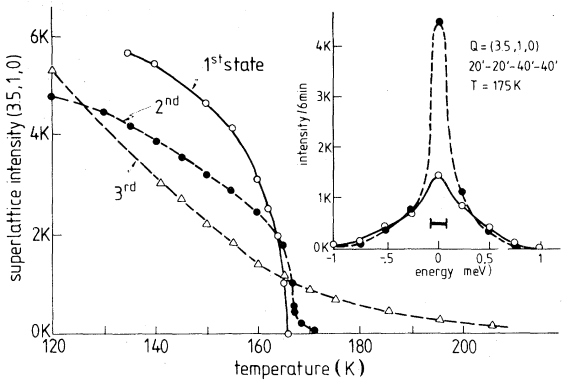

FIG. 4. Temperature dependence of superlattice intensity which signalizes the doubling of the a axis (Ref. 10). The parameter is the degree of conversion. The third state corresponds to the autocatalytic region. The inset shows inelastic broadening of the critical scattering.

metry and in the last case even an indication of a doubly peaked structure. Another remarkable observation is the strong intensity variation within the sheets. With the energy resolution of about 0.4 meV no inelasticity of the diffuse sheets could be detected.

C. Acoustic modes

In agreement with Brillouin scattering results,[9] an increase of the acoustic velocities is observed. The biggest effect occurs for the longitudinal acoustic mode along the b direction. Here the sound velocity increases from 2.96×10^5 cm/sec for 13% conversion to 3.98×10^5 cm/sec in the third state. These values result in about 15% conversion rather than the nominal 13% and in about 50% conversion rather than 60%, when compared to the Brillouin measurement.[9] No attempt was made for a systematic measurement of elastic constants.

D. Phase transition

X-ray structure investigations by Enkelmann and Wegner[10] have revealed a phase transition at about 170 K which is accompanied by a doubling of the lattice parameter a due to a twisting of the side groups of the TS molecule. Robin *et al.*[6] have detected that there exists an intermediate incommensurate phase between 206 and 163 K for the monomer state which is not present in the polymer state. Here the cell doubling occurs at about 206 K. An even more complicated picture emerges from recent calorimetric studies.[11] Our contribution to the phase diagram is depicted in Fig. 4. We observe via superlattice intensity the cell doubling at about 166 K for the first state of conversion (about 13%). With increasing conversion to the third state the transition is smeared out. Possibly this behavior reflects a distribution of T_c due to local strain. The inset of Fig. 4 shows an inelastic broadening above T_C but no underdamped soft phonon at about 10° above T_C. Since the phase transition is a special property of PTS and seems not to be directly related to the polymerization process, no systematic investigation was attempted.

In contrast to the previous x-ray results[12] which showed a smooth variation of the b-lattice parameter with polymerization, the neutron data show b to change discontinuously. Furthermore, the diffuse sheets showed correspondingly asymmetric profiles. It was therefore decided to undertake a more detailed examination of these effects by polymerizing the third crystal in smaller steps. The location of the seven investigated states of polymerization on the polymerization curve is indicated in Fig. 2 by the symbols A to G. The scattering plane contained the (020) and $(40\bar{2})$ reflections and corresponds closely to the a,b plane of the real lattice. Figure 5(a) shows the conversion dependence of the (020) reflection by means of a scan along the b^* (or b) direction. The state D clearly exhibits a doubly peaked structure. In order to check whether the crystal contained large regions of different degree of polymerization, the diffracted neutron beam was photographed in both peak positions. If the crystal contained macroscopic region of inhomogeneously polymerized material, this would show up as alternate bright and dark regions in the two diffraction photographs. No evidence for such behavior was present in the photographs. "Mosaic averaged" scans for the state D are displayed in Fig. 5(b) for various temperatures. They show that the lattice expansion along b is essentially due to the larger ("monomer") distance whereas the shorter ("polymer") distance remains nearly constant. The thermal expansion coefficient for the "monomer" distance $b_0^{-1}\Delta b/\Delta T =$ is 0.92, 0.89, 0.76, 0.75×10^{-4}

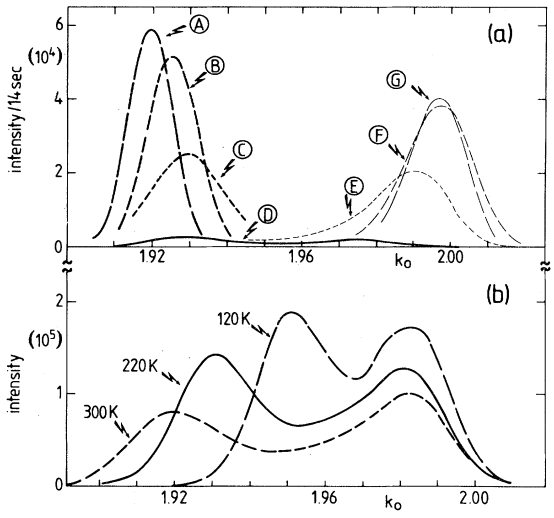

FIG. 5. (a) Conversion dependence of (020) reflection. k_0 in units for the polymer state. *A* to *G* see Fig. 2. (b) "Mosaic averaged" (020) reflection for state *D* at different temperatures.

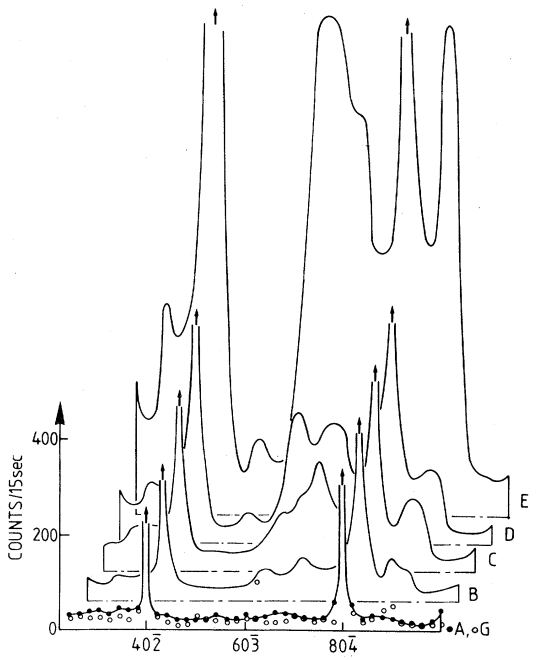

FIG. 6. Growth and decay of zeroth sheet intensity. The state *F* is omitted for clearness of presentation.

deg^{-1} for the state *A,B,C,D*, respectively, and about 0.07×10^{-4} deg^{-1} for the "polymer" distance.

Analogous scans (along b^*) of other Bragg reflections display even more complicated structures. The conclusions which may be drawn from these observations about the distribution of intermolecular "equilibrium" distances (along *b*) in the autocatalytic region (state *D*) are as follows: There is more than one "lattice parameter" *b*; its distribution is broad and displays two main and some minor peaks; the various observed peaks are not associated with macroscopic domains of the sample and may deviate slightly (about 0.5°) from the main direction of *b*; the resolution limited interference volume extends over about 80 molecules along the *b* axis and about 50 molecules along the *a* axis.

The second object of a more detailed examination was the behavior of diffuse sheets. To this end a complete mapping of the accessible and relevant regions of reciprocal space was done for states *A* and *G*. Examples of the growth and decay of the diffuse sheets are given in Figs. 6 and 7 (zeroth and third sheets, respectively). The most striking observations are: (a) There is a strong modulation of intensity within the sheets; (b) the intensity of the zeroth sheet is of the same order of magnitude as that of other sheets; (c) on comparing the widths of the zeroth and third sheets, one finds the latter width is greater and has an asymmetric profile. Furthermore, the long tail of the profile occurs at $k < 3$ at small degree of polymerization and at $k > 3$ for nearly complete polymerization. At intermediate polymerization (state *D*) the sheet appears doubled. The intensity modulation does not necessarily mean that the interaction between the chains along *b* is strong, since even for the isolated chain a strong modulation is expected due to the form factor of the molecule. The existence of a zeroth sheet is in contrast to similar systems, where the disorder occurs along chains, too. No zeroth sheet is observed, e.g., for the one-dimensional ionic conductor $LiAlSiO_4$ (Ref. 13) or the one-dimensional "liquid" $Hg_{3-g}AsF_6$.[14]

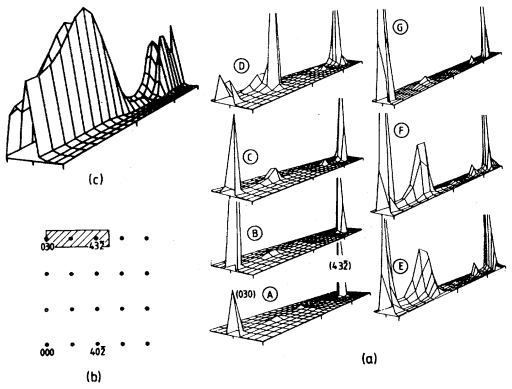

FIG. 7. (a) Development of third sheet intensity with conversion. (b) Portion of reciprocal space displayed in (a). (c) Model calculation for 60% conversion and 90% cluster probability.

II. ELASTIC SCATTERING FROM CHAIN ARRAY

The elastic scattering $S(\vec{Q})$ is given by the Fourier transform of the average scattering density correlation function

$$S(\vec{Q}) = \langle \hat{\rho}(\vec{Q})\hat{\rho}(-\vec{Q}) \rangle \ ,$$

where $\rho(\vec{r})$ is the scattering density and $\vec{Q}$ means the momentum transfer of the scattered particle. Writing $\rho(\vec{r})$ as sum of chain (label j) contributions, one has for a regular array of chains ($||, \perp$ refer to chain direction)

$$\rho(r) = \sum_{j}^{N_j} \rho^{(j)}(\vec{r}_{||})\delta(\vec{r}_{\perp} - \vec{r}_{\perp}^{(j)}) \ .$$

It is instructive to decompose the density of a chain into an average part and the deviation (disorder)

$$\rho^{(j)}(\vec{r}_{||}) = \langle \rho(\vec{r}_{||}) \rangle + \delta\rho^{(j)}(\vec{r}_{||}) \ .$$

Then $S(\vec{Q})$ splits into the following three contributions:

$$S(\vec{Q}) = \Delta^2(\vec{Q}_{\perp}) \langle \hat{\rho}(\vec{Q}_{||}) \rangle \langle \hat{\rho}(-\vec{Q}_{||}) \rangle + N_j \langle \delta\hat{\rho}^{(0)}(\vec{Q}_{||})\delta\hat{\rho}^{(0)}(-\vec{Q}_{||}) \rangle + \sum_{j \neq j'} \langle \delta\hat{\rho}^{(j)}(\vec{Q}_{||})\delta\hat{\rho}^{(j')}(-\vec{Q}_{||}) \rangle \exp[i\vec{Q}_{\perp} \cdot (\vec{r}_{\perp}^{(j)} - \vec{r}_{\perp}^{(j')})] \ , \quad (1)$$

where

$$\Delta^2(\vec{Q}_{\perp}) = \sum_{j,j'} \exp[i\vec{Q}_{\perp}(\vec{r}_{\perp}^{(j)} - \vec{r}_{\perp}^{(j')})]$$

represents the two-dimensional Bragg condition resulting from the regular array of chains. The first term in Eq. (1) describes the usual three-dimensional (3D) array of Bragg reflections in the extreme case where $\langle \rho(\vec{r}_{||}) \rangle$ is given by a periodic delta function. In the other extreme where $\langle \rho(\vec{r}_{||}) \rangle = \text{const}$ one gets Bragg reflections merely in the basal plane ($Q_{||} = 0$). The second term in Eq. (1) is independent of $\vec{Q}_{\perp}$, and thus describes "sheets" of scattering intensity originating from the self-correlation of the disorder on a single chain. The third term represents the correlation of the disorder between different chains.

III. MODEL FOR DISORDER

By polymerization, the initially perfect monomer crystal becomes disordered, reaches a state of maximum disorder around 50% conversion, and becomes again a perfectly ordered state upon complete conversion (polymer crystal). To extract the essential information, provided by the neutron measurements, we would like to model this complicated process on a tractable level. Although the model is too simple, one might expect to get some insight into the actual disorder by examination of the deficiencies.

The basis for the model is provided by structural information obtained from x-ray analysis. Figure 1 shows those results. The unit cell contains two stacks of molecules along the monoclinic axis b which are related by the glide plane of space group $P2_1/c$. Molecules adjacent along the stack (or chain) direction b are linked together by a covalent bond upon polymerization as shown in Fig. 1(b). Thereby the intermolecular distance and the shape of the molecule is changed. This information suggests the following description of the crystal density. A two state variable $\sigma = \pm 1$ labels the shapes of a molecule, where $\sigma = +1$ signifies that the molecule is part of a polymerized unit, otherwise $\sigma = -1$. The molecular distance along b may be given by $d_{\pm}$ for adjacent spins $\sigma_n = \sigma_{n+1} = \pm 1$. For distances between polymerized and unpolymerized regions (different signs of the spins) one might introduce a third length d_0. However, since the covalent forces are much stronger than the van der Waals interactions we have simplified further by setting $d_0 = d_- =$ monomer distance. In a first approximation we have also assumed that the polymerization process proceeds independently on each chain and the problem becomes one dimensional.

IV. SINGLE-CHAIN CONTRIBUTION

The scattering density is given by

$$\rho(\vec{r}) = \sum_{m,\kappa} b_{\kappa}\delta(\vec{r} - \vec{r}_{m,\kappa}) \ ,$$

where m labels the molecules along a chain and κ labels the atoms within a molecule, b_{κ} is the scattering length. Denoting the position of the inversion center of a molecule by y_m one may write

$$\vec{r}_{m,\kappa} = y_m\vec{e}_{||} + \vec{s}_{\kappa}(\sigma m) \ .$$

Here $\vec{e}_{||}$ is a unit vector along the chain and $s_{\kappa}(\sigma_m)$ represents the two sets of atomic positions within the molecular coordinate system referring to the polymer ($\sigma_m = +1$) and the monomer ($\sigma = -1$) shape of the molecule. Defining a molecular density $\rho_+(y)$ and a spin density $\rho_-(y)$ by

$$\rho_+(y) = \sum_m \delta(y - y_m) \ ,$$

$$\rho_-(y) = \sum_m \sigma_m\delta(y - y_m) \ ,$$

one may write the Fourier transform of the scattering density

$$\hat{\rho}(Q) = \langle f \rangle \hat{\rho}_+(Q_\parallel) + \delta f \hat{\rho}_-(Q_\parallel)$$

with the molecular structure factor

$$f(\sigma_m) = \sum_\kappa b_\kappa \cos[\vec{Q} \cdot \vec{s}(\sigma_m)]$$

and

$$\left.\begin{matrix} \langle f \rangle \\ \delta f \end{matrix}\right\} = \tfrac{1}{2}[f(+) \pm f(-)] \ .$$

There remains the task to evaluate the expectation values of the spin and molecular density and their correlation. To this end we define the probability for a spin configuration $\{\sigma\}$ of the chain[15]

$$P(\{\sigma\}) = \langle s|\sigma_n\rangle \langle \sigma_n|\underline{M}_0|\sigma_{N-1}\rangle \langle \sigma_{N-1}|\underline{M}_0 \ldots \underline{M}_0|\sigma_2\rangle \times \langle \sigma_2|\underline{M}_0|\sigma_1\rangle \langle \sigma_1|g\rangle \ .$$

$\underline{M}_0$ denotes a two state Markov matrix

$$\underline{M}_0 = \begin{pmatrix} p' & p \\ \bar{p}' & \bar{p} \end{pmatrix}; \quad p' + \bar{p}' = p + \bar{p} = 1$$

with $p'(p)$ being the probability to toss a + sign if the foregoing result was a +(−) sign. Equivalently, one may use the language of the Ising chain [nearest-neighbor (NN) interaction J, field H] with the correspondence

$$\exp(4\beta J) = \frac{p'\bar{p}}{p\bar{p}'}; \quad \tan\delta\beta H = \frac{p - \bar{p}'}{p' + \bar{p}} \ .$$

The boundary conditions are chosen for convenience to be

$$|g\rangle = (p + \bar{p}')^{-1} \begin{pmatrix} p \\ \bar{p}' \end{pmatrix}; \quad \langle s| = (1, 1)$$

with

$$\underline{M}_0|g\rangle = |g\rangle; \quad \langle s|\underline{M}_0 = \langle s| \ .$$

With these probabilities for the spin configurations, the various correlation functions are given by $(v, v' = \pm 1)$

$$\langle \hat{\rho}_v(Q_\parallel)\hat{\rho}'_{v'}(-Q_\parallel)\rangle = \sum_{m=1}^{N} \sum_{m'=1}^{N} \langle v|M^{m-m'}|v'\rangle \ ,$$

where

$$\underline{M} = \begin{pmatrix} p'y_+ & py_0 \\ \bar{p}'y_0 & \bar{p}y_- \end{pmatrix}$$

takes into account the correct phase factor between adjacent molecules by setting

$$y_{\underset{0}{\pm}} = \exp(iQ_\parallel d_{\underset{0}{\pm}})$$

and v labels spin and molecular density with the notation

$$|\pm\rangle = \begin{pmatrix} 1 & 0 \\ 0 & \pm 1 \end{pmatrix} |g\rangle; \quad \langle \pm| = \langle s| \begin{pmatrix} 1 & 0 \\ 0 & \pm 1 \end{pmatrix} \ .$$

Since in general the absolute of the eigenvalues of the transfer matrix $\underline{M}$ are smaller than unity, there arises no convergence problem for the infinitely long chain $(N \to \infty)$ and the geometric series may be summed up to

$$\langle \hat{\rho}_v(Q_\parallel)\hat{\rho}'_v(-Q_\parallel)\rangle = N\{\langle v|v'\rangle + \langle v|\underline{M}(\underline{I} - \underline{M})^{-1}|v'\rangle + \langle v'|\underline{M}^*(\underline{I} - \underline{M}^*)^{-1}|v\rangle\} \ ,$$

where $\underline{I}$ denotes the unit matrix.

This expression describes—besides the form factors $\langle f \rangle$ and δf—the sheet intensity, since $\langle \hat{\rho}_v \rangle \langle \hat{\rho}_{v'} \rangle$ is by a factor N^{-1} smaller than the above. The factor N^{-1} expresses the nonexistence of long-range order in the one-dimensional model. An exception is the zeroth sheet where $\langle \hat{\rho}_v \rangle \langle \hat{\rho}_{v'} \rangle$ cancels the forward scattering.

Denoting the eigenvalues of $\underline{M}$ by $\lambda_{1,2}$ one may write alternatively

$$\underline{M}(\underline{I} - \underline{M})^{-1} = (1 - \lambda_1)^{-1}(1 - \lambda_2)^{-1}[\underline{M} - \underline{I}\det(\underline{M})] \ ,$$

which shows that the diffuse sheets emerge for values of $Q_\parallel$ where one of the eigenvalues comes close to 1. It is obvious that there may result double sheets if both eigenvalues pass through "resonance" for neighboring values of $Q_\parallel$. This is the case if

$$[\mathrm{tr}(\underline{M})]^2 \approx 4\det(\underline{M}) \ ,$$

which means—not too surprisingly—the region of large clusters $(p' - p \approx 1)$. (The opposite limit $p' - p = 0$ reduces to the familiar binomial distribution.)

A demonstration of this situation is given in Fig. 7(c) which shows the calculated intensity for the third sheet. The parameters are as follows: clustering $\rho = p' - p = 0.9$, conversion $u = p(p + \bar{p}')^{-1} = 0.6 d_-/d_+ = 1.03$ and $d_- = d_0$. The molecular form factor was taken from Kobelt and Paulus[16] for the "polymer" molecule. For the "monomer" molecule only the backbone carbons were rearranged according to the structure analysis of Enkelmann *et al.*[2,12] The slight twisting of the side-groups and Debye-Waller factors have been omitted for this demonstration. The latter results in an overestimation of the intensity for larger momentum transfers. Although the calculation contains essentially only one parameter—the cluster parameter ρ—there is at least qualitative agreement with the observations in state D. The basis for the estimate of ρ was the appearance of a double sheet for $k = 3$. Thus the value of $\rho = 0.9$ is a lower limit for the clustering

tendency. The expectation values of polymer (+)– and monomer (–)–cluster length in terms of u and ρ are given by ($\bar{u}=1-u$)

$$l_+=\bar{u}^{-1}(1-\rho)^{-1}l_-=u^{-1}(1-\rho)^{-1} \ .$$

Thus the calculation corresponds to an expected length of polymer cluster of 25 molecules, which is in reasonable agreement with the analysis of Brillouin scattering data by Enkelmann *et al.*[12]

The zeroth sheet for the array of uncorrelated chains corresponds to the small angle scattering in the three-dimensional case. Its intensity is determined by the

$$\lim_{Q_{\parallel}\to 0}\langle\hat{\rho}_\nu(Q_{\parallel})\hat{\rho}'_\nu(-Q_{\parallel})\rangle$$

which is obtained by expanding $\underline{M}$ into powers of $Q_{\parallel}$:

$$\underline{M}=\sum_{k=0}^{\infty}(iQ_{\parallel})^k/k!\,\underline{M}_k \ .$$

The result for the correlation of the molecular density is

$$\langle f\rangle^2 N^{-1}\lim_{Q_{\parallel}\to 0}\langle\hat{\rho}_+\hat{\rho}_+^*\rangle = \left[\frac{(\delta d)^2}{\langle d\rangle^2}+\frac{2}{1-\rho}\frac{(\tilde{\delta d})^2}{\langle d\rangle^2}\right]\langle f\rangle^2 \ ,$$

where the fluctuations of the intermolecular distance are given by

$$(\delta d)^2=\langle\underline{M}_2\rangle-\langle\underline{M}_1\rangle^2 \ ,$$

$$(\tilde{\delta d})^2=\langle\underline{M}_1^2\rangle-\langle\underline{M}_1\rangle^2 \ ,$$

with $\langle d\rangle=\langle\underline{M}_1\rangle$ and $\langle\ldots\rangle=\langle s|\ldots|g\rangle$.

These relative fluctuations are small (order of 10^{-4}) and correspond to the compressibility limit of the scattering by liquids. In contrast to the Hg chains[14] they may be enhanced considerably for PTS by strong "ferromagnetic" clustering ($\rho\to+1$).

In the other extreme ($d_-=d_-=d_0$) one has form factor fluctuations only and the intensity of the zeroth sheet is determined by

$$(\delta f)^2 N^{-1}\lim_{Q_{\parallel}\to 0}\langle\hat{\rho}_-\hat{\rho}_-^*\rangle=4u\bar{u}\frac{1+\rho}{1-\rho}(\delta f)^2 \ .$$

This is the well-known description for the small angle scattering from "ferromagnetic" domains. For β-eucryptite[13] there is a strong "antiferromagnetic" clustering ($\rho\to-1$) and therefore this contribution to the zeroth sheet is small. For PTS this term gives the main contribution to the zeroth sheet in state D and it reflects the difference between the form factors for the monomer and polymer molecule.

CONCLUSIONS

The neutron scattering experiment on PTS confirms results obtained by x rays and Brillouin scattering.[6,9,12] Since neutrons do not cause polymerization, additional information could be obtained by passing through the autocatalytic region in small steps. The development of large internal strain manifests itself by a broad mosaic distribution and by a "smeared out" phase transformation. The tremendous decrease of the (020) reflection signals the loss of long-range order along the b direction (direction of polymerization). The distribution of the lattice parameter b develops at least two peaks and doubled diffuse diffraction sheets occur. The Ising model seems helpful for a least qualitative understanding of the independent chain features. Its translation into the scattering density is somewhat unusual since spin orientation and position are strongly coupled.

The increase of the chain interaction becomes visible in states E and F (Fig. 6) by an enhancement of the sheet intensity at multiples of the reciprocal-lattice vector (1,0,-0.5) which corresponds to a next neighbor chain interaction along the crystallographic a direction. Such an enhancement is to be expected for a weakly interacting chain array which is describable by solving "exactly" the one-dimensional behavior and treating the chain coupling in mean-field approximation.[17] The complexity of the data prevents us from pursuing this aspect further.

ACKNOWLEDGMENTS

We are grateful to G. Wegner and H. H. Stiller for stimulating the experiment and to V. J. Emery, for helpful discussions. H.G. thanks the staff at Brookhaven National Laboratory for the hospitality during his stay there. Work at Brookhaven was supported by the Division of Basic Energy Sciences, Department of Energy, under Contract No. DE-AC02-76-CH00016.

---

*Visiting scientist appointment on leave from Institut für Festkörperforschung Kernforschungsanlage Jülich, 5170 Julich, Federal Republic of Germany now returned.

[1]G. Wegner, Z. Naturforsch. Teil B 24, 824 (1969). See also: R. H. Baughman, J. Appl. Phys. 43, 4362 (1972); D. Bloor, L. Koski, G. C. Stevens, F. H. Preston, and D. J. Ando, J. Mater. Sci. 10, 1678 (1975).

[2]V. Enkelmann and G. Wegner, Angew. Chem. 89, 432 (1977).

[3]K. Lochner, T. Hinrichsen, W. Hofberger, and H. Bässler,

Phys. Status Solidi (a) 50, 95 (1978).
[4]G. N. Patel, R. R. Chance, E. A. Turi, and Y. P. Khana, J. Am. Chem. Soc. 100, 6644 (1978).
[5]G. Wegner, in *Molecular Metals,* edited by W. H. Hatfield (Plenum, New York, 1979), p. 209ff.
[6]P. Robin, J. P. Pouget, R. Comés, and A. Moradpour, J. Phys. (Paris) 41, 415 (1980).
[7]C. Kröhnke, V. Enkelmann, and G. Wegner, Chem. Phys. Lett. 71, 38 (1980).
[8]V. Enkelmann, R. J. Leyrer, and G. Wegner, Makromol. Chem. 180, 1787 (1979).
[9]R. J. Leyrer, W. Wettling, and G. Wegner, Ber. Bunsenges, Phys. Chem. 82, 697 (1978).
[10]V. Enkelmann and G. Wegner, Makromol. Chem. 178, 635 (1977).
[11]M. Bertault, P. Collet, and M. Schott, J. Phys. (Paris) (March, 1981) (in press).
[12]V. Enkelmann, R. J. Leyrer, and G. Wegner, Makromol. Chem. 180, 1787 (1979).
[13]W. Press, B. Renker, H. Schulz, and H. Böhm, Phys. Rev. B 21, 1250 (1980).
[14]I. D. Brown, B. D. Cutforth, C. G. Davies, R. J. Gillespie, P. R. Ireland, and J. E. Vebries, Can. J. Chem. 52, 791 (1974).
[15]See, e.g., R. V. Mises, *Mathematical Theory of Probability and Statistics* (Academic, New York, 1964).
[16]D. Kobelt and E. F. Paulus, Acta Crystallogr. Sect. B 30, 232 (1974).
[17]D. J. Scalapino, Y. Imry, and P. Pincus, Phys. Rev. B 11, 2042 (1974).